Effect of mixing metakaolins: methodological approach to estimate metakaolin reactivity

W. N'Cho, A. Gharzouni, Jenny Jouin, A. Aimable, I. Sobrados, S. Rossignol

Effect of mixing metakaolins: methodological approach to estimate metakaolin reactivity

W. N'cho[1], A. Gharzouni[1], J. Jouin[1,*], A. Aimable[1], I. Sobrados[2], S. Rossignol[1]

[1] *IRCER: Institute for Research on Ceramics (UMR CNRS 7315), European Center for Ceramics, 12 rue Atlantis 87068 Limoges Cedex, France.*

[2] *Instituto de ciencia de materiales de Madrid, Consejo superior de investigaciones científicas (CSIC), C/Sor Juana Inés de la Cruz, 3, 28049 Madrid, Spain.*

** Corresponding author: sylvie.rossignol@unilim.fr*

Abstract

Geopolymers are obtained from an alkali silicate solution and aluminosilicate sources. The source commonly used geopolymer is metakaolin. The chemical composition, extraction site or calcination process of metakaolin influence its reactivity and thus the properties of the consolidated samples. This work focused on clarifying how the properties of aluminosilicate-based raw materials evolve when different metakaolin sources are mixed. The study involved mixing different metakaolins to evaluate their physico-chemical properties. The different samples were characterized by measuring their granulometry, wettability and zeta potential. Structural data were obtained from X-ray diffraction and ^{27}Al nuclear magnetic resonance spectroscopy. It appears that the properties of the mixtures can be expressed as a function of different parameters. Granulometric properties directly depend on the quantity of each source, wettability is related to the amount of available amorphous aluminum in the sources, and zeta

potential is strongly influenced by the source with the highest amount of siliceous-based impurities. This methodological approach can be applied to geopolymer synthesis.

Keywords: granulometry, wettability, impurities, zeta potential, XRD, NMR

I Introduction

The development of new building materials that promote lower energy consumption and environmental preservation remains a global challenge. In this domain, geopolymeric materials are attracting increasing interest because their synthesis methods are relatively simple and they exhibit a low environmental impact is low, high thermal and mechanical performances [1, 2], and wide range of applications [3]. Geopolymers are described as amorphous 3D networks that can sometimes present crystalline phases, such as quartz and illite [4,5]. These materials are obtained from the activation of an aluminosilicate source by an alkali-based solution or acidic-based solution [6, 7, 8]. The consolidation of these materials occurs at temperatures below 100 °C [9].

The most commonly used aluminosilicate sources are metakaolin. They are generated from the dehydration and deshydroxylation of kaolinite by a thermal treatment [10]. Different authors have studied the thermal production of metakaolins from kaolinite. The goal is to obtain the formation of 4-fold- and 5-fold-coordinated aluminum from the original 6-fold-coordinated aluminum, as they are more reactive for geopolymer synthesis [11]. This can be determined and followed using nuclear magnetic resonance spectroscopy [12]. The optimized calcination temperature of the raw material ranges between 600 and 800 °C; above these temperatures, the crystallization of mullite ($3Al_2O_3{\cdot}2SiO_2$) occurs at approximately 1150 °C [12]. Many features of metakaolins have been determined to try to predict the key parameters that influence their

reactivity toward geopolymerization and thus their final working properties. Among these, the calcination process, the granulometric features, and specific surface have been studied and linked to their reactivity. The flash calcination process leads to reactivities and appears more attractive because it is faster and less expensive compared to rotary furnace calcination [13,14]. However, the works of A. Gharzouni et al. [15] provide evidence that the heat treatment of argillite in a furnace rotary between 700 and 800 °C leads to the complete dehydroxylation of clay minerals (illite–smectite, illite/mica, kaolinite and chlorite) and to the total transformation of octahedral aluminum into tetrahedral aluminum and chlorite), whereas the flash process induces partial structural dehydroxylation of the clay minerals, regardless of the temperature [15]. Indeed, it was shown that calcination induced in a rotary furnace led to the formation of massive aggregates of particles. In contrast, flash calcination produced finer, less agglomerated and potentially more reactive particles [16]. To improve the reactivity, some aluminosilicate sources, wastes or by-products, and metakaolin can be added to concrete [17, 18]. G. Barone et al. [17] showed that replacing 10-25% metakaolin with volcanic ash in the synthesis of activated alkali materials leads to an increase in compressive strength. Another study by E. Tiffo et al. [18] showed that geopolymers based on metakaolin or alkali-activated volcanic slag can reach thermally stable products at 1150 °C with high compressive strengths. Similarly, Z. A. Hasan et al. [19] showed that for concrete production, the combination of metakaolin and ash improves properties at fresh state.

According to Fabbri *et al.* [20], a large specific surface did not necessarily guarantee a high reactivity of metakaolin, as the deshydroxylation led to the formation of porous grains in which the small pores could be penetrated by nitrogen gas but not by water. The wettability, or water demand, also seems to be strongly correlated to the reactivity of metakaolin, as a high

wettability is often measured with highly reactive metakaolin. Studies conducted by A. Autef et al. [11] have shown the importance of the wettability parameter to evaluate the reactivity of metakaolins. Finally, other parameters, such as the amount of crystalline impurities (quartz, muscovite), the composition and the presence of tetrahedral aluminum, have been designed as key parameters. In summary, several studies [4, 5, 8] have shown that reactive metakaolins are typically characterized by low Si/Al molar ratios (≤ 1.2) and high values of wettability (≥ 760 µl/g), amorphous phase (≥ 63 %) and proportion of reactive tetrahedral aluminum (≥ 19 %) [21].

Notably, the reactivity, which is related to the dissolution rate of the aluminosilicate source in the activating solution, involves surface charges. Indeed, the surface charges in clay minerals are essential for understanding the behavior of clay species in acidic or basic media and evaluating their reactivity [22, 23, 24, 25, 26]. A study on the dispersion and the zeta potential of pure clays performed by M. Chorom *et al.* [27] revealed that the surface charges were the main factor controlling the dispersion of clay. Many researchers have thus worked on the electrokinetic properties of clay minerals, including kaolinite. Among them, Huertas *et al.* [28] studied the dissolution rate of kaolinite by measuring the silicate and aluminous species released into solution over a range of pH values from 1 to 13. This work revealed that kaolinite dissolves at pH < 4 and pH > 11 and that the release of aluminous species decreases at pH values between 5 and 10 due to the precipitation of $Al(OH)_3$ [29, 30]. Moreover, at pH > 12, the dissolution of kaolinite was higher than that in acidic media [28]. These results corroborate knowledge that aluminous sites are more highly charged in basic media and therefore more reactive than silicate sites [29]. Moreover, the siloxane surface and the aluminol surface, named basal faces, are noncharged, whereas the edges present hydroxyl groups Al-OH and Si-OH and thus either

positive or negative charges depending on the pH [31]. This surface charge heterogeneity, also described by a patchy model, was originally presented by Van Olphen [32] and has since been confirmed by many authors [33, 34]. This leads to the simultaneous presence of negatively and positively charged parts on the surface of clay mineral particles under acidic conditions, although the overall particle charge is negative. Studies have revealed that the zeta potential of kaolinite varies from -25 mV (pH = 3) to -42 mV (pH = 11) [26]. Finally, some researchers have demonstrated that metakaolin dissolves more readily in alkaline media than uncalcined kaolin [35] due to the crystalline destruction of kaolinite and releases more aluminous and silicate species in solution. The high concentration of these species causes supersaturation of the solution, which leads to the precipitation of an aluminum-rich gel [36].

The reactivity and properties of aluminosilicate sources, such as metakaolins, have been thoroughly studied in the literature. However, few studies have been conducted on the properties of mixed metakaolin sources and their influence on the resulting geopolymer properties. This can be an issue since the variability of the sources is high and mixing can occur when performing very large-scale syntheses. It is thus important to develop a methodological approach to determine how a mixture of metakaolins reacts with the activating source. The goal of this work was thus to study different metakaolins and then characterize their mixtures to understand their behavior.

II Experimental part

1. Raw materials and sample preparations

A selection of three aluminosilicate sources was chosen for this work, and the details are listed in Table 1. Metakaolin M5 was supplied by Argeco (Fumel, France), while metakaolin

M1 and kaolinite KI were provided by Imerys (Clerac, France). The kaolin KI was calcined in a rotary furnace at 750 °C for 90 min with a heating and cooling rate of 5 °C.min^{-1}, resulting in the metakaolin, which was further denoted as MI. The idea was to utilize metakaolins with different purities. M5 and M1 metakaolins contain impurities, whereas MI is a pure metakaolin. Furthermore, M1 and M5 metakaolins are used very frequently in France. M5 is obtained by flash calcination, whereas M1 and MI are obtained by rotary furnace calcination. Finally, a 5 M potassium silicate solution (S), as used by Scanferla et al. [37], was used to prepare consolidated samples.

The three metakaolins were mixed following the compositions reported in Figure 1. After weighing the raw materials, they were blended for 30 min at 45 rpm using a Turbula mixer. The obtained mixtures, as well as the raw metakaolins, were then characterized to determine the evolution of their properties. Finally, bulk samples were synthetized using the S solution and consolidated at room temperature to verify whether these mixtures led to the formation of geopolymers; all the samples managed to consolidate.

2. Characterization

The granolumetric distributions of the samples were measured with a Horiba Ltd. LA-950 laser particle size analyzer (Kyoto, Japan). In this method, particles scatter light at a defined angle depending on their size. The produced pattern was then analyzed using the Fraunhofer-Kernel method to obtain the particle size distribution. Specific surfaces of the powders were quantified by the BET method (Brunauer, Emmett and Teller). The measurements were realized using a Micrometrics Tristar II 3020 device (Norcross, USA). Samples of approximately 2 g were degassed for 12 hours at 90 °C prior to characterization.

The wettability value, or water demand, corresponds to the volume of water that can be adsorbed by one gram of powder before saturation [21]. This value was evaluated by weighing one gram of powder in a glass cup, then using a micropipette, water was added to the powder microliter by microliter until visual saturation of the granular assembly. Zeta potential is the electric potential developed at the shear plane of a particle dispersed in a liquid medium. The evolution of the zeta potential was monitored as a function of the pH. First, a suspension of 0.25 g of the sample was dispersed in 25 mL of distilled water by using a sonotrode for 90 s with 3 s intermittence. Then, the measurement of zeta potential was carried out with a Colloid Metrix Stabino II zetameter (Meerbusch, Germany). The pH was modified using normadose (1 M) solutions of HCl and NaOH by adding a 15 µL volume of solution every 20 s. Initially, all metakaolin and mixture suspensions possessed a natural pH between 5 and 7.

The mineralogy of the samples was identified by X-ray diffraction (XRD) on a Bruker D8 Advance diffractometer using CuKα radiation. The data were collected over a 2θ angular range of 5-60° with a step size of 0.02° and an equivalent measured time per step of 57 s. The crystalline phases were identified from the experimental patterns using the powder diffraction file (PDF) database of the International Center for Diffraction Data. Before measurement, the samples were mechanically crushed and sieved (50 µm). Finally, the amorphous rate of different metakaolin diffractograms was evaluated by Peakoc software. This method is generally referred to as the absolute method of determining the degree of crystallinity. It consists of calculating the ratio between the total intensity of the lines of all crystallized minerals present in the sample and the total diffracted intensity (including the amorphous dome). The formula is transposed to determine the amorphous dome, and thus the amorphous content can be calculated [38].

High-resolution MAS-NMR experiments were performed at room temperature on a Bruker Avance - 400 spectrometer operating at 104.26 MHz for ^{27}Al. MAS experiments were carried out for metakaolin MI, M1, M5 and MIM1 samples, which were spun at 10 kHz. Four hundred scans were carried out with a 2 µs pulse width and a period between successive accumulations of 5 s. Chemical shift values were given with respect to an external aqueous $AlCl_3$ solution. The deconvolution of the central part of the spectra, using Gaussian/Lorentzian models, was then realized with the DMFIT program software [39]. considering that metakaolin is amorphous, quadrupolar shapes are not well defined, and the lateral bands are not very visible. For this reason, the fits were made with Lorentzian/Gaussian components.

III Results

1. Physico-chemical properties of the aluminosilicate sources

Figure 2 displays the volumetric particle size distribution for the different metakaolins and one mixture (MIM5). The whole data, which illustrate the distributions measured for all mixtures, can be found in the supplementary material. The distributions are different, which illustrates the great diversity of aluminosilicate sources that can be used to form geopolymers. The size distribution of MI (Figure 2a) reveals a single population centered at approximately 10 µm in diameter. This particle diameter is typical of pure metakaolin, as observed by Gharzouni *et al.* [21]. M1 (Figure 2b) is characterized by a multimodal distribution of grain sizes. Three main contributions can be distinguished, which are centered at 3 µm, 10 µm and 35 µm. As demonstrated in previous work, they can be attributed to muscovite, metakaolin and quartz, respectively [21]. Although the quartz phase represents a large portion of the volume fraction of the sample, the phase is limited to a small number of particles, which limits their

eventual reactivity in the system; as a result, the particles play the role of mechanical reinforcement in consolidated materials [5]. Finally, M5, in Figure 2c, displays a bimodal distribution, with metakaolin grains with diameters centered at approximately 10 µm and larger quartz-type grains at 80 µm in diameter.

The granulometric distribution of the MIM5 mixture is represented as an illustration in Figure 2d. It corresponds to the sum of the granulometric distribution of MI and M5. Indeed, contributions at 10 µm and 100 µm, corresponding to metakaolin-type clay and quartz, were already present in the unmixed samples MI and M5. The same observations were made for the other mixtures, as shown in the supplementary material. This confirms that, from a granulometric point of view, mixing two (or more) different metakaolins does not modify their properties, which remain an average of the original properties. The values of population diameters, measured on the volume distribution for all samples, are reported in Table 2. The variability of the obtained measurements, especially for the highest values, reveals the large differences originating from the extraction pit of the kaolinites. Once again, the diameter values of mixtures correspond to the average diameter of starting metakaolins, showing that mixing meatakaolins barely exerts an influence on their final granulometry. Indeed, the contribution from the "pure" metakaolin (at approximately 10 µm) is clearly visible, as well as the eventual presence of impurities.

The specific surfaces of the samples were measured prior to and after mixing. The values are presented in Table 2. These specific surface area values vary from 7 to 17 m^2/g for the starting metakaolins, providing evidence that the particles available for the polycondensation reaction are different due to the disparity in impurity size for the three sources of MI, M1 and M5 metakaolins. This behavior can affect the dissolution of metakaolins by inducing different

behaviors [7]. These values are in agreement with existing data [21]. When mixed, the measured specific surface corresponds roughly to the average of the starting values. This confirms that mixing the metakaolins does not lead to aggregation or consolidation of the particles.

The wettability values of all samples can also be found in Table 2. They vary from 530 µL/g for M5 to 1200 µL/g for MI. The wettability is closely related to the metakaolin's ability to react in alkaline media, as shown by Gharzouni *et al.* [21] for other sources. Unsurprisingly, the wettability values of the mixtures range between the values of the starting raw materials. However, the data do not provide fully relevant information about the mixtures, as they are composed of heterogeneous grains, and thus, the geopolymerization reaction depends on their different populations. Moreover, the measured wettability of a mixture is not simply the average of the starting wettability values, as was the case for a specific surface, for example. Thus, a more suitable parameter may needs to be defined to describe the evolution of this property, and the nominal composition is not sufficient.

Finally, the zeta potential as a function of the pH was measured for all samples. A selection of the obtained curves can be found in Figure 3, and their totality is available in the supplementary material. Moreover, their minimum values are reported in Table 2.

First, the evolution of the zeta potential as a function of the pH is similar for all the measured samples. Indeed, the samples exhibit the same general evolution, from a maximum of 0 to 6 mV to a minimum of -45 to -85 mV before increasing again, with their main difference being their minimum value. The values remain negative for the most part; the isoelectric point (IEP), indicating the pH for which the zeta potential equals zero, is situated at a pH value of approximately 2. Moreover, the point of maximum negative charge of the particles is reached in the alkaline zone at pH ~ 11 before the zeta potential values increase sharply toward 0 mV.

More precisely, for the metakaolin MI represented in Figure 3a, the modification of zeta potential during the acidification of the medium by progressive addition of the HCl solution into the suspension initially at pH = 6.5 causes a progressive increase in the zeta potential until reaching the IEP at a pH value of 2. Then, the zeta potential remains constant despite the further decrease in the pH values. Concerning the measurement in alkaline medium, the progressive addition of the NaOH solution into the suspension leads to a decrease in the zeta potential until a minimum value of -85 mV is reached for a pH value of approximately 11. Then, a sharp increase occurs when additional NaOH solution is added, tending toward zero. These observations are valid for all samples, with the exception of M1, which shows a positive zeta potential value (~ 6 mV) for a small pH range of approximately 2 before reaching back to zero. The evolution of the zeta potentials of all metakaolins for pH values between 2 and 11 is similar to the results obtained in studies concerning kaolinite [26, 40]. However, at pH=11, the observed zeta potential of kaolinite (-42 mV) is higher than the values obtained in this study for dehydroxylated kaolinite, suggesting a better dispersion of the particles [26]; this partially occurs due to the destruction of the kaolin structure after calcination [35]. At extreme pH values (pH < 2 and pH > 11), the evolution of zeta potentials corresponds with the results obtained by M. Chorom *et al.* [27], who explained these observations using the double layer theory; this theory stipulates that compression of the double layer is caused by the increase in the concentration of electrolytes in the system, which favors a decrease in the values of zeta potential [27, 41]. The other samples have a similar evolution (Figure 3b and c), and their only difference seems to be the value of the negative charge surface that is reached at pH = 11. These values are reported in Table 3 and are equal to -85, -75 and -46 mV for the MI, M1 and M5 samples, respectively. These differences observed between the minimum zeta potential values

of the metakaolins at pH = 11 can be related to the mineralogy of the materials. Indeed, the results of the particle size distribution and impurity identification revealed that MI presents a single population composed solely of clay minerals, whereas M1 and M5 each present multiple populations composed of quartz and clay minerals for the most part. The highest amount of impurities is in M5, which shows the lowest absolute value of the surface charge; thus, there seems to be a relation between this value and the amount of silica-based impurities in the sample. When mixing metakaolins, the shapes of the curves remain the same, and only the value of the minimum is sensitive to the composition of the sample. However, for the zeta potential, the minimum value reached by the mixture is far from the average zeta potential of the starting compounds. Indeed, the minimum zeta potential for the M1M5, MIM5 and M1MIM5 mixtures is almost equal to the value of M5, and the minimum value of the MIM1 mixture is very close to that of M1. This suggests that for a mixture, one metakaolin governs the zeta potential of the sum. In all cases, the governing source shows the most siliceous-based impurities, and the dispersion of particles depends on its mineralogy.

Finally, to clarify the evolution of properties, such as wettability and zeta potential, which does not simply follow the nominal composition of samples, further characterizations were conducted on the samples to determine their amount of impurities and reactive aluminum.

2. Determination of the reactive aluminum rate

The mineralogical composition of the samples was determined using XRD measurements. First, the diffractograms of MI, M1 and M5 can be seen in Figure 4. They all show the presence of a large amorphous hump as well as peaks corresponding to crystalline phases. The amorphous contribution, which is positioned at approximately 23° in all the samples, is the signature of the part denoted as pure metakaolin [42]. Indeed, previous works [21, 39] have

validated that the amorphous content of metakaolins is a potential indicator of their reactive part. This contribution is more or less visible depending on the level of impurities contained in the sample. For example, MI is almost entirely composed of amorphous metakaolin and can be considered a reference material for geopolymerization. The crystalline impurities depend largely on the extraction pit of the metakaolin. All of them present peaks characteristic of the quartz (Q) and anatase (A) phases. In addition, M1 contains muscovite (M) and kaolinite (K), and the latter indicates that the deshydroxylation of kaolinite induced by the thermal treatment performed by the producer was incomplete. M5 presents some calcite (Ca) and hematite (H) contributions, which are caused in particular by the rich ferrous nature of the ground it was extracted from and can easily be noticed by the reddish hue of M5. The identification of the crystalline phases was then followed by quantitative analysis of the amorphous contribution in the samples using the area ratio method [38]. Prior to the calculation, the areas of the peaks were determined using Peakoc software with a Voigt function, taking into account the $K_{\alpha 1}$-$K_{\alpha 2}$ doublet of the Cu wavelength emission. The calculated amorphous amounts of the samples are reported in Table 3. Regardless of the metakaolin or mixture, the amorphous contents range from 44 to 98 %. Concerning the starting metakaolins, MI shows the highest amorphous content, followed by M1 (56 %) and M5, which exhibits with the lowest amorphous content (44 %). This gives an estimation of the amount of impurities; “pure” metakaolin, which contains the reactive part of the sample, is amorphous. When mixing the metakaolins, the XRD diagrams of the samples correspond to the sum of the diagrams of the starting metakaolins. Indeed, this method is volume sensitive, and crystalline impurities are maintained in the mixtures. The amorphous rate follows the same rule, i.e., it corresponds to the average of the amorphous part

measured on the starting metakaolins. No modification of the crystalline state of the sample is thus induced by the blending, as could be expected by the stability of the previous properties.

Among the samples, differently coordinated aluminum can be found. The ^{27}Al NMR study of metakaolins and mixtures was thus conducted to identify the quantity of each sample and the calculation of the reactive aluminum rate in each sample. This was achieved through identifying the different peaks corresponding to the presence of hexacoordinated, pentacoordinated, and tetracoordinated aluminum from the ^{27}Al NMR spectra of the different metakaolins and the MIM1 mixture, as shown in Figure 5. All metakaolin spectra display three main peaks at approximately 55, 27 and 2 ppm and are assigned to $Al^{(IV)}$, $Al^{(V)}$ and $Al^{(VI)}$ aluminum, respectively [21, 43, 44, 45]. The intensities of these contributions differ largely for each metakaolin. Indeed, MI presents a large peak for $Al^{(V),}$ while M1 is particularly $Al^{(VI)}$-rich. The spectra of the MIM1 mixture seem to present the contributions from each aluminum, with their intensity being roughly the sum of the two starting metakaolins. To facilitate the exploitation of the spectra, deconvolutions of the central part were performed, as seen in Figure 6 for M1, for example. The complete deconvolution results are reported in Table 4. The different contributions are confirmed to be present in every sample, with the exception of the ~18 ppm contribution, which is attributed to $Al^{(V)}$; this could be found in MI only and the mixtures containing MI. Bands at 55, 27 and -5 ppm are characterized by a large broadening and full width at half maximum (FWHM) between 25 and 35. This reflects the structural disorder of the metakaolin. The 2-ppm contribution is narrower (FWHM≈12) and is assigned to crystalline material. This is in good agreement with the XRD identification. From these data, the different coordinated aluminum rates were determined for each metakaolin as well as for the MIM1 mixture. The relative intensities of each contribution are different for each metakaolin, as seen

in the spectra. Moreover, the relative intensities of each contribution in the M1MI mixture are close to the average of the contributions from each starting metakaolin.

Using the previous results obtained both by XRD and NMR, the reactive aluminum rates for the metakaolins and mixtures were determined. The results are presented in Table 5. For this calculation, $Al^{(IV)}$ and $Al^{(V)}$ were categorized as reactive, while $Al^{(VI)}$ was not [21]. The reactive aluminum rates of the mixtures that were not measured by NMR were estimated on the basis of the observations described for M1MI. As could be supposed from the wettability values, MI showed the highest amount of reactive aluminum (64%) followed by M5 (26%) and finally M1 exhibited the lowest amount (26%). These results are in good agreement with those of Gharzouni *et al.* [21,39].

IV Discussion

The methodological approach of a given metakaolin mixture is essential for controlling their reactivity and, later, the working properties of the geopolymer obtained from this mixture. Correlations between the properties of the mixtures and some controlling parameters thus need to be determined.

In this work, it first appeared that some properties can be directly deduced from the volume fraction of each starting compound. This is the case in particular for granulometric data and specific surfaces, as represented in Figure 7a. The specific surfaces presented in this ternary diagram indeed reveal values of 7, 17 and 12 m^2/g for MI, M1 and M5, respectively. The values measured for all mixtures correspond to the average of the reference metakaolins. Likewise, the prediction for the quantity of pure amorphous metakaolin in the mixture can be performed by a simple sum of the volume fraction of pure metakaolin in the starting materials (Figure 7b). It

seems that all types of metakaolin can be mixed without interference. In these cases, the effect of starting metakaolin impurities seems to provide no influence despite the large difference in crystallinity between them.

Then, it appeared that some key properties, such as wettability, that were used to determine the reactivity of the aluminosilicate sources were not directly related to the volume fraction of the raw materials. Wettability is a parameter for evaluating the content of aluminum and siliceous species in metakaolin [8]. In this case, the correlation parameter had to be determined. It seems that the wettability of the samples is linked with the availability of amorphous aluminum, which was estimated from the previous structural data. The resulting parameter, defined as $amorphous\ rate \times composition\left(\frac{Al}{Si}\right)$, was used as a variable in Figure 8 to plot the evolution of wettability in metakaolins and mixtures. The linear correlation is good, considering the error in the wettability measurement. This parameter considers the chemical composition of the sample and the presence of quartz, for example, as well as the inherent dispersibility of each metakaolin. The latter does change depending on the extraction site or thermal treatment used to transform kaolinite in amorphous raw material. It seems that the calcination process influences the wettability of metakaolins. Indeed, metakaolin M5, which has the lowest wettability value, is obtained by flash calcination, whereas metakaolins M1 and MI obtained by rotary furnace calcination show higher wettability values, which suggests that metakaolins obtained by flash calcination have a low water demand. These results are in accordance with the literature [15]. For such properties, it seems that the presence of tetrahedral- or pentahedral-coordinated aluminum only plays a minor role in the correlation, and the availability of amorphous aluminum is critical, regardless of its environment. Notably, the highly reactive

metakaolins exhibited a high amorphous rate (> 63%) and a wettability higher than 760 µl/g, as determined by Gharzouni *et al.* [8].

Finally, it appeared that some properties of metakaolin mixtures were not sensitive to the quantity of each term within the mixture. The example of zeta potential measurement is especially clear in this case. All the metakaolins and mixtures exhibited the same global behavior as a function of the pH, but the minimum value of the zeta potential of the particles in the suspensions was systematically determined by the raw material with the lowest value. This is summarized in Figure 9, in which the red zone corresponds to the mixtures involving M5 (M1M5, MIM5, MIM5M1), the dark gray zone involves M1 and no M5 (M1, M1MI) and the light gray is pure MI. The zeta potential is the lowest for metakaolins with the lowest amount of crystalline impurities (as seen from their amount of amorphous phase), but this correlation does not apply when dealing with mixtures. In this case, regardless of the number of raw materials or their respective amount, the zeta potential of the mixture is governed by the presence of metakaolin with the lowest charge value, which was M5 in this work. If no M5 was involved, then the raw material affecting the value of the zeta potential was M1. This limits the quality of the resulting suspension dispersion [27] and reveals the sensitivity of the zeta potential to the impurities contained in the starting metakaolins.

Conclusion

In this work, the study of raw metakaolins and mixtures, both in terms of physico-chemical and structural properties, helped clarify the influence of starting raw materials on the properties of mixtures.

First, it was determined that the granulometric features and specific surfaces are a direct function of the volume fraction of each raw metakaolin. Then, to understand the evolution of

wettability, which is closely related to the reactivity of the source, the amount of reactive aluminum in the samples was determined. The wettability of the mixture was then defined as a function of the available amorphous aluminum in the metakaolins. Finally, the dispersion of the mixture, correlated to the zeta potential, did not seem to comply with any kind of mixture rule. In this case, the mineralogy, and the amount of silica-based impurities in particular, limited the zeta potential values to the lowest absolute value.

Through this methodological approach, we can estimate the reactivity of metakaolin mixtures by determining the characteristics of the raw materials. Work on geopolymer synthesis followed by evaluation of use properties, such as mechanical testing and porosity, will now be necessary to verify the transferability of the reactivity of metakaolin mixtures to geopolymers.

Acknowledgments

The authors wish to thank the Nouvelle Aquitaine region (*Céramiques géopolymères à temperature ambiante pour différentes applications* - 2018) for its financial support.

References

[1] M. Arnoult, M. Perronnet, A. Autef, G. Gasgnier, S. Rossignol, *Impact of various aluminosilicate compounds in geopolymer foam formation to a Si/M=0.7 of silicate solution*, eramic Engineering and Science Proceedings, **38[3]** (2018) 191-200.

[2] P.Duxson, J.L. Provis, G.C. Lukey, S.W. Mallicoat, W.M. Kriven, *Understanding the relationship between geopolymer composition, microstructure and mechanical properties*, Colloids Surf., A Physicochem. Eng. Asp., **269** (2005) 47-58.

[3] J.L. Provis, J.S.J. van Deventer, *Geopolymer, Structure, Processing and Industrial Applications*, Woodhead Publishing Ltd (2009)

[4]L. Weng, K. Sagoe-Crentsil, T. Brown, S. Song, *Effects of aluminates on the formation of geopolymers*, Materials Science and Engineering: B., **117** (2005) 163-168.

[5] A. Autef, E. Joussein, A. Poulesquen, G. Gasgnier, S. Pronier, I. Sobrados, J. Sanz, S. Rossignol, *Influence of metakaolin purities on potassium geopolymer formulation: The existence of several networks*, J. Colloids and Interface Sci., **408** (2013) 43-53.

[6] E. Prud'homme, E. Joussein, C. Peyratout, A. Smith, S. Rossignol, *Consolidated geo-materials from sand or industrial waste*, Ceram. Eng. Sci., **30** (2010) 314-324.

[7] A. Autef, E. Joussein, G. Gasgnier, S. Rossignol, *Feasibility of aluminosilicate compounds from various raw materials: Chemical reactivity and mechanical properties*, Powder Technol., **301** (2016) 169-178.

[8] A. Gharzouni, E. Joussein, B. Samet, S. Baklouti, S. Rossignol, *Effect of the reactivity of alkaline solution and metakaolin on geopolymer formation*, J. Non-Cryst. Solids., **410** (2015) 127-134.

[9] J. Davidovits, *Inorganic Polymeric New Materials*, Journal of Thermal Analysis, **37** (1991) 1633-56.

[10] K.L. Koffi, J. Soro, J.Y.Y. Andji, S. Oyetola, G. Kra, *Etude comparative de la déshydroxylation/amorphisation dans deux kaolins de cristallinité différente*, J. Soc. Ouest-Afr. Chim., **30** (2010) 29-39.

[11] A. Autef, E. Joussein, A. Poulesquen, G. Gasgnier, S. Pronier, I. Sobrados, *Role of metakaolin dehydroxylation in geopolymer synthesis*, Powder Technol., **250** (2013) 33-39.

[12] J. Rocha, J. Klinowski, *Solid-state NMR studies of the structure and reactivity of metakaolinite*, Angewandte Chemie International Edition in English, **29[5]** (1990) 553-554.

[13] S.Salvador, Pozzolanic properties of flash-calcined kaolinite: A comparative study with soak-calcined products, Cement and Concrete Research Volume 25, Issue 1, (1995) 102-112.

[14] R.San Nicolas, M.Cyr, G.Escadeillas Characteristics and applications of flash metakaolins, Applied Clay Science Volumes 83–84, (2013), 253-262.

[15] A.Gharzouni, C.Dupuy, I.Sobrados, E.Joussein, N.Texier-Mandoki, X.Bourbon, S.Rossignol The effect of furnace and flash heating on COx argillite for the synthesis of alkali activated binders, Journal of Cleaner Production 156 (2017) 670-678.

[16] V. Medri, S. Fabbri, J. Dedecek, Z. Sobalik, Z. Tvaruzkova, A. Vaccari, *Role of the morphology and the dehydroxylation of metakaolins on geopolymerization*, Appl. Clay Sci., **50** (2010) 538-545.

[17] G. Barone, C. Finocchiaro, I. Lancellotti, C.Leonelli, P. Mazzoleni, C. Sgarlata, A. Stroscio, Potentiality of the Use of Pyroclastic Volcanic Residues in the Production of Alkali Activated Material, Waste and Biomass Valorization (2021) 12:1075–1094.

[18] E. Tiffo, P. D. Belibi Belibi, J. B. Bike Mbah, A. Thamer, T. Ebenizer Pougnong, J. Baenla, A. Elimbi, Effect of various amounts of aluminium oxy-hydroxide coupled with thermal treatment on the performance of alkali-activated metakaolin and volcanic scoria, Scientific African 14(2021) 01015.

[19] Z.A. Hasan, M. S. Nasr, M.K. Abed, Properties of reactive powder concrete containing different combinations of fly ash and metakaolin. Materials Today: Proceedings, 42, (2021), 2436-2440.

[20] B. Fabbri, S. Gualtieri, C. Leonardi, *Modifications induced by the thermal treatment of kaolin and determination of reactivity of metakaolin*, Appl. Clay Sci., **73** (2013) 2-10.

[21] A. Gharzouni, I. Sobrados, E. Joussein, S. Baklouti, S. Rossignol, *Control of polycondensation reaction generated from different metakaolins and alkaline solutions*, J. Ceram. Sci. Technol., **08[3]** (2017) 365-376.

[22] Y. Gu and D. Li, *The ζ -potential of glass surface in contact with aqueous solutions*, J. Colloid Interface Sci., **226** (2000) 328-339.

[23] L.J. West and D.L. Stewart, *Effect of Zeta potential on soil electrokinesis*, The proc. of Geoenvironment, ASCE, Boulder, CO, (2000), 535-1549.

[24] B. Lorne, F. Perrier, J. Avouac, *Streaming potential measurements 1. Properties of the electrical double layer from crushed rock samples*, J. Geophys. Res., **104** (1999) 17857-17877.

[25] I. Sondi, J. Biscan, V. Pravdic, *Electrokinetics of pure clay minerals revisited*, J. Colloid Interface Sci., **178** (1996) 514-522.

[26] Y. Yukselen A. Kaya, *Zeta potential of kaolinite in the presence of alkali, alkaline earth and hydrolyzable metal ions*, Water, Air, and Soil Pollution, **145** (2003) 155-168.

[27] M. Chorom, P. Rengasamy, *Dispersion and zeta potential of pure clays as related to net particle charge under varying pH, electrolyte concentration and cation type*, European Journal of Soil Science, **46** (1995) 657-665.

[28] F.J. Huertas, L. Chou, R. Wollast, *Mechanism of kaolinite dissolution at room temperature and pressure Part II: Kinetic study*, Geochimica et Cosmochimica Acta, **63[19]** (1999) 3261-3275.

[29] A. Bauer and G. Berger, *Kaolinite and smectite dissolution rate in high molar KOH solutions at 35 and 80°C*, Applied Geochemistry, **13[7]** (1998) 905-916.

[30] F.K. Crundwell, *The mechanism of dissolution of minerals in acidic and alkaline solutions: Part II Application of a new theory to silicates, aluminosilicates and quartz*, Hydrometallurgy, **149** (2014) 265-275.

[31] E. Tombácz and M. Szekeres, *Surface charge heterogeneity of kaolinite in aqueous suspension in comparison with montmorillonite*, Applied Clay Science, **34[1]** (2006) 105‑124.

[32] H. Van Olphen, *An introduction to clay colloid chemistry*, vol. 97. Interscience, New York (1964).

[33] Z. Zhou and W. D. Gunter, *The nature of the surface charge of kaolinite*, Clays Clay Miner., **40[3]** (1992) 365‑368.

[34] B. K. Schroth and G. Sposito, *Surface charge properties of kaolinite*, Clays Clay Miner., **45[1]** (1997) 85‑91.

[35] M.A. Longhi, E.D. Rodríguez, S.A. Bernal, J.L. Provis, A.P. Kirchheim, *Valorisation of a kaolin mining waste for the production of geopolymers*, Journal of Cleaner Production, **115** (2016) 265-272.

[36] A. Fernández-Jiménez, A. Palomo, I. Sobrados, J. Sanz, *The role played by the reactive alumina content in the alkaline activation of fly ashes*, Microporous and Mesoporous Materials, **91[1-3]** (2006) 111-119.

[37] P. Scanferla, A. Gharzouni, N. Texier-Mandoki, X. Bourbon, S. Rossignol, *Effects of potassium-silicate, sands and carbonates concentrations on metakaolin-based geopolymers for high-temperature applications*, Open Ceramics, **10** (2022) 100257.

[38] M. Cyr, B. Husson, A. Carles-Gibergue, *Détermination, par diffraction des rayons X, de la teneur en phase amorphe de certains matériaux minéraux*, J. Phys. IV France, **08-PR5** (1998) Pr5-23-Pr5-30.

[39] A. Gharzouni, I. Sobrados, E. Joussein, S. Baklouti, S. Rossignol, *Predictive tools to control the structure and the properties of metakaolin based geopolymer materials*, Colloids Surf. A Physicochem. Eng. Asp., **511** (2016) 212-221.

[40] G. Sposito, *The Chemistry of Soils*, Oxford University Press, New York, (1989).

[41] P. Fievet, A. Szymczyk, C. Labbez, B. Aoubiza, C. Simon, A. Foissy, J. Pagetti, *Determining the zeta potential of porous membranes using electrolyte conductivity inside pores*, Journal of Colloid and Interface Science, **235** (2001) 383-390.

[42] V. Mathivet, J. Jouin, A. Gharzouni, I. Sobrados, H. Celerier, S. Rossignol et M. Parlier, *Acid-based geopolymers: understanding of the structural evolutions during consolidation and after thermal treatments*, Journal of non crystalline solids, **512** (2019) 90-97.

[43] I.W.M. Brown, K.J.D. Mackenzie, M.E. Bowden, R.H. Meinhold, Outstanding problems in the kaolinite-mullite reaction sequence investigated by ^{29}Si and ^{27}Al Solid-state Nuclear Magnetic Resonance: II, High-temperature transformations of metakaolinite, J. Am. Ceram. Soc., **68** (1985) 298-301.

[44] P. Duxson, G.C. Lukey, F. Separovic, J.S.J. van Deventer, *Effect of alkali cations on Aluminum incorporation in geopolymeric gels*, Ind. Eng. Chem. Res., **44** (2005) 832--839.

[45] M.R. Rowles, J.V. Hanna, K.J. Pike, M.E. Smith, B.H.O. Connor, *^{29}Si,^{27}Al, ^{1}H and ^{23}Na MAS NMR study of the bonding character in aluminosilicate inorganic polymers*, Appl. Magn. Reson., **32** (2007) 663-689.

Table 1: Nomenclature and composition of the different raw materials.

Name	Provider	Weight composition (%)	Heating process
M5	ARGECO	SiO_2: 59.9 Al_2O_3:35.3	Flash
M1	IMERYS	SiO_2: 55.0 Al_2O_3:40.0	Rotary furnace – 750 °C
KI		SiO_2: 54.0 Al_2O_3:46.0	Calcined to MI in a rotary furnace at 750 °C

Table 2: Chemical and physical properties of the starting metakaolins and mixtures, i.e., nominal composition, granulometric characteristics, specific surface, wettability and minimum value of zeta potential

Samples	Nominal aluminum (%mol)	Pop.1 (µm)	Pop.2 (µm)	Pop.3 (µm)	BET (m^2/g)	Wettability (µL/g)	Minimum values of zeta potential (mV)
MI	0.50	-	10	-	7	1200	-85
M1	0.46	3	9	35	17	740	-75
M5	0.40	-	10	80	12	530	-46
MIM1	0.48	2	10	75	11	850	-76
MIM5	0.45	-	10	100	10	780	-50
M1M5	0.43	3	10	100	15	620	-47
MIM1M5	0.44	2	9	100	12	700	-47

Table 3: Amorphous rate of metakaolins and mixtures.

Samples	**Experimental amorphous rate (%, ±1)**	**Calculated amorphous rate (%, ±1)**
MI	98	-
M1	56	-
M5	44	-
M1MI	79	*77*
MIM5	72	*71*
M1M5	48	*50*
M1MIM5	67	*66*

Table 4: ^{27}Al NMR data of the various aluminum species for raw metakaolins and M1MI

Samples		Percentage of the area curve of contribution (%)				
		Al^{IV}	Al^{V}		Al^{VI}	
MI	*Contribution*	≈ 54 ppm **20%**	≈ 30 ppm **37%**	≈ 18 ppm **8%**	≈ 1.8 ppm **15%**	≈ -5 ppm **20%**
	FWHM	25	25	15	14	35
M1	*Contribution*	≈ 57 ppm **18%**	≈ 26.5 ppm **27%**	-	≈ 2 ppm **30%**	≈ -5 ppm **25%**
	FWHM	28	30	-	11	35
M5	*Contribution*	≈ 54 ppm **26%**	≈ 26.5 ppm **33%**	-	≈ 2 ppm **19%**	≈ -5 ppm **22%**
	FWHM	25	26	-	12	35
MIM1	*Contribution*	≈ 55.5 ppm **18%**	≈ 30.0 ppm **33%**	≈ 16 ppm **8%**	≈ 2.3 ppm **20%**	≈ -7 ppm **21%**
	FWHM	25	25	15	12	35

Table 5: reactive Al rate of metakaolins and mixtures

Samples	**Aluminum contributions (%)**			**Amorphous contribution (%)**	**Reactive Al rate (%)**
	Al^{IV}	Al^{V}	Al^{VI}		
MI	20	45	35	98	64
M1	18	27	55	56	26
M5	26	33	41	44	26
M1MI	18	41	41	79	47
MIM5	*23*	*39*	*38*	72	*45*
M1M5	*22*	*30*	*48*	48	*26*
M1MIM5	*21*	*35*	*44*	67	*38*

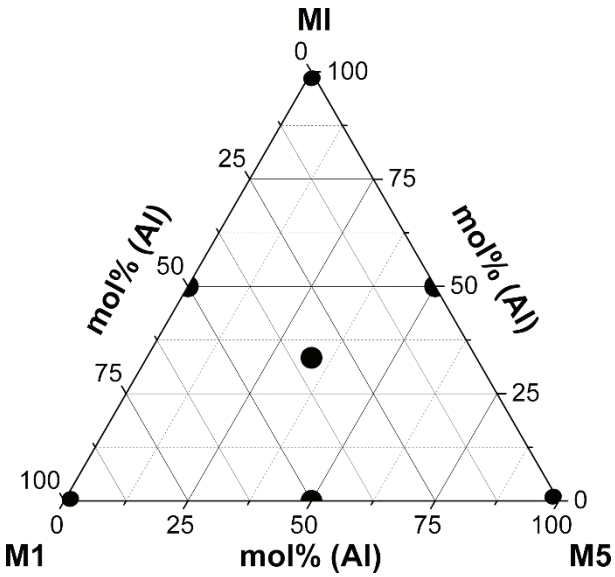

Figure 1: Selected raw metakaolins and prepared mixtures.

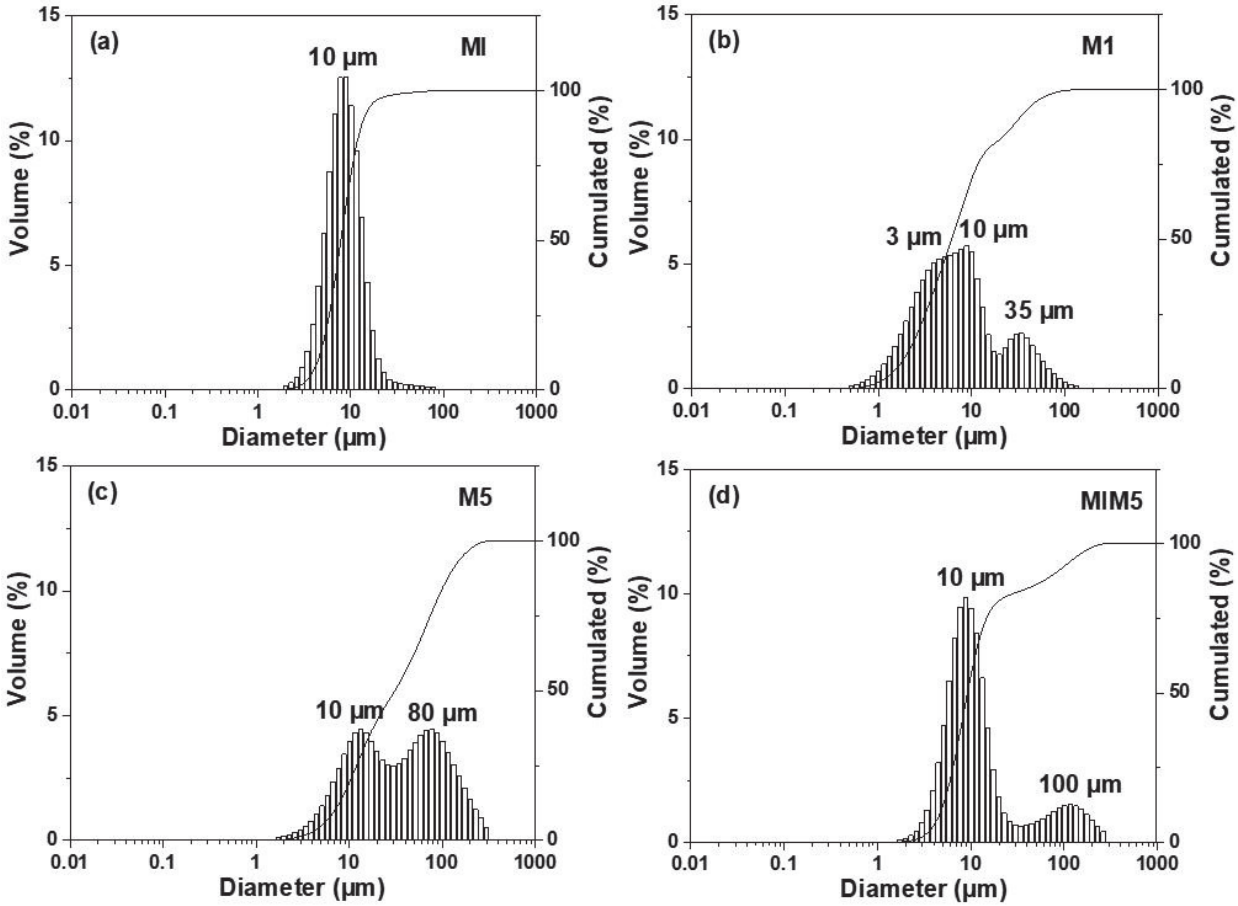

Figure 2: Volume distribution of particles in pure metakaolins MI (a), M1 (b), M5 (c), and mixed sources MIM5 (d).

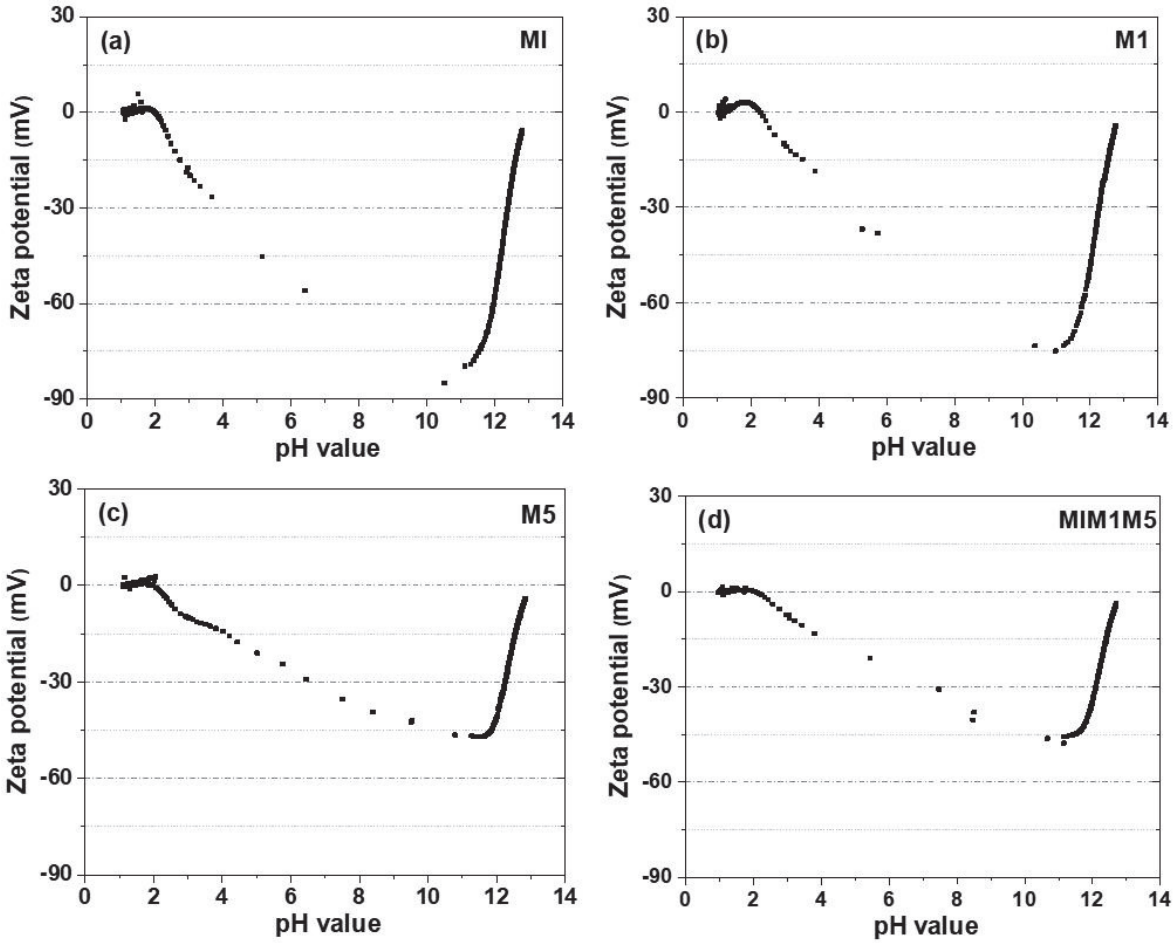

Figure 3: Evolution of metakaolin zeta potentials as a function of the suspension pH values for (a) MI, (b) M1, (c) M5 and (d) MIM1M5.

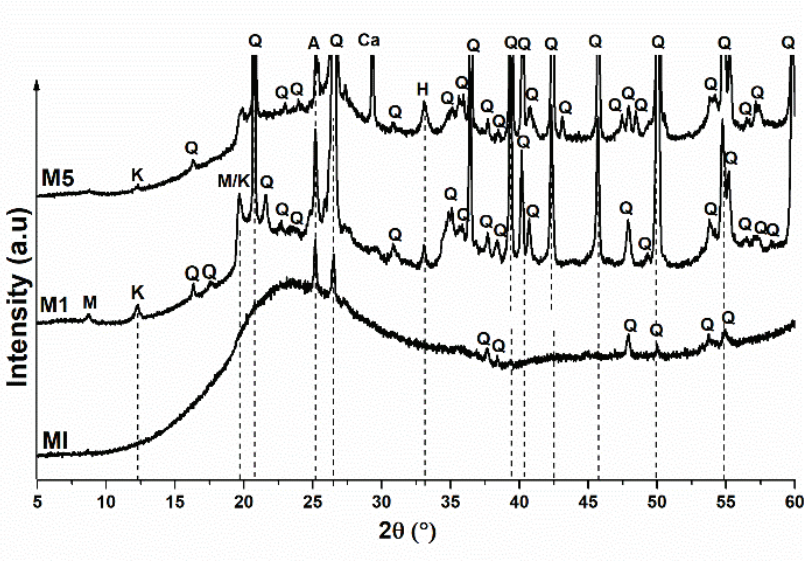

Figure 4: Diffractograms of MI, M1 and M5 metakaolin samples. The crystalline phases are identified as follows: Q: quartz (01-083-2465), M: muscovite (00-003-0849), K: kaolinite (00-012-0447), A: anatase (01-071-1166), Ca: calcite (00-005-0586), and H: hematite (01-079-1741).

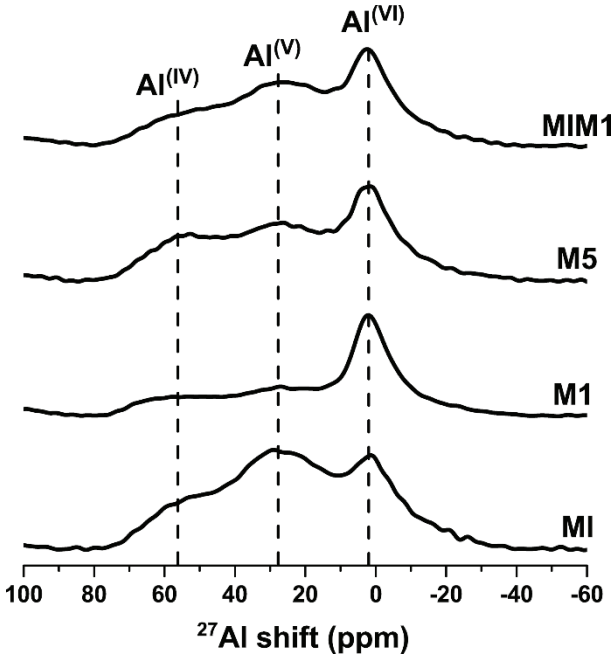

Figure 5: ^{27}Al NMR spectra of the raw metakaolins and mixture MIM1

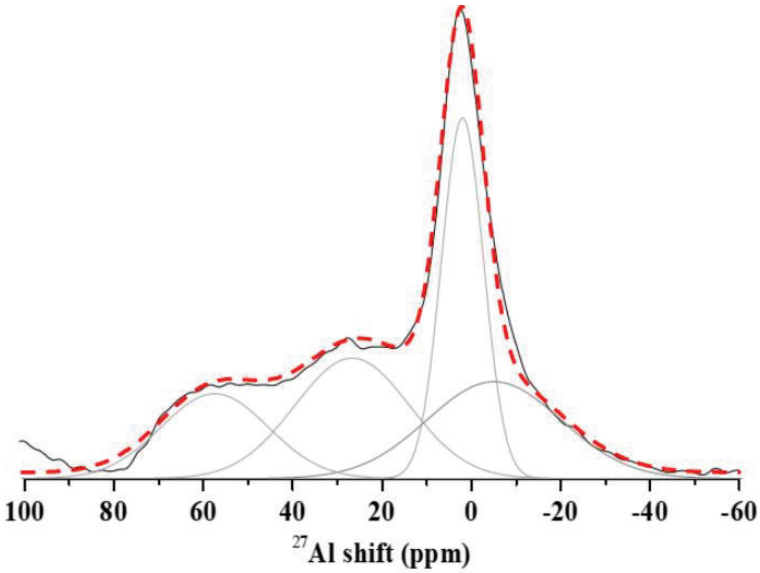

Figure 6: Example of deconvolution performed on the NMR spectrum of M1. Calculated (

- - - -), experimental (——), contributions (——)

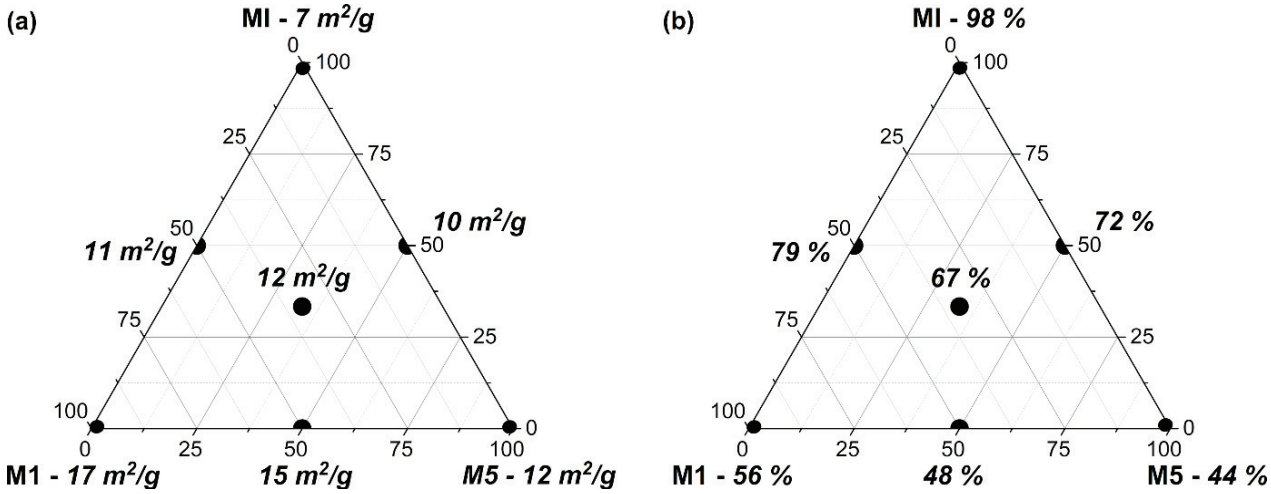

Figure 7: Representation of the (a) specific surface and (b) amorphous rate of pure metakaolins and mixtures.

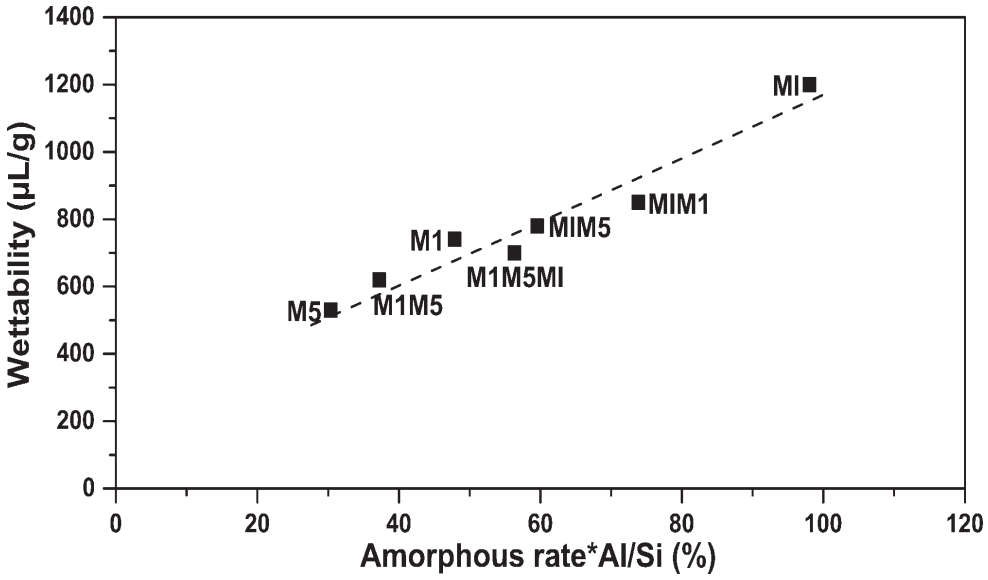

Figure 8: Evolution of wettability of metakaolins and mixtures as a function of the reactive aluminum composition of the source.

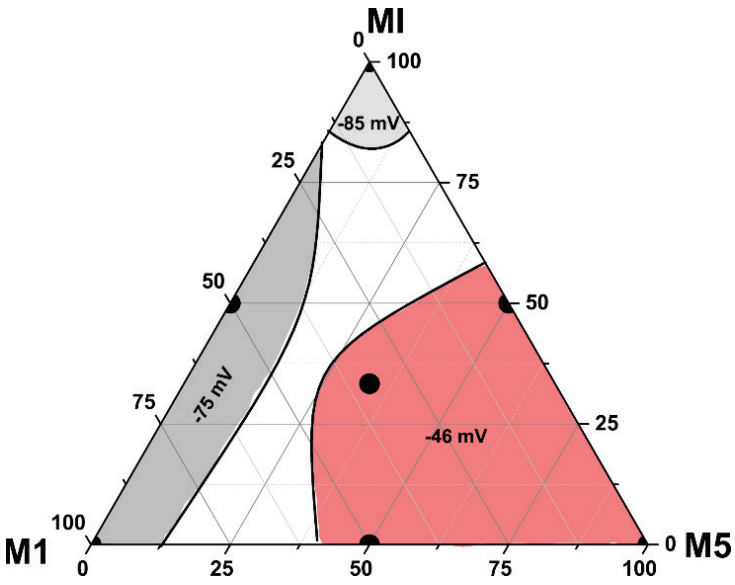

Figure 9: Minimum measured values of zeta potential (highest surface charge) for water-based suspensions of metakaolins and selected mixtures